

Prediction and measurement of perpendicular giant magnetoresistances of Co/Cu/Ni₈₄Fe₁₆/Cu multilayers

Q. Yang, P. Holody, R. Loloee, L. L. Henry, W. P. Pratt, Jr., P. A. Schroeder, and J. Bass
*Department of Physics and Astronomy and Center for Fundamental Materials Research, Michigan State University,
 East Lansing, Michigan 48824-1116*

(Received 12 October 1994)

We show that a simple two-current model gives good predictions of the low-temperature perpendicular (CPP) specific resistances, AR_t (A = sample area, R_t = sample resistance), of sputtered Co/Cu/Py/Cu (Py = Ni₈₄Fe₁₆ ≈ permalloy) multilayers with neighboring Co and Py layers in well-defined parallel (P) or antiparallel (AP) magnetic states, using only parameters derived without adjustment from prior measurements on Co/Cu and Py/Cu multilayers.

In addition to its intrinsic interest, the phenomenon of giant (G) negative magnetoresistance (MR) in magnetic multilayers composed of alternating layers of a ferromagnetic (F) and a nonmagnetic (N) metal is being examined for a variety of technological uses.¹ The ability to tailor systems for specific uses requires understanding the physics underlying GMR. Demonstrating the ability to predict new data from old is an important step along the path of understanding.

At low temperatures, description of the usual current in plane (CIP) MR in F/N multilayers involves two characteristic lengths, the elastic mean free paths for momentum transfer in the F and N metals. These lengths appear as exponential factors that greatly complicate analysis.^{2,3}

In contrast, the characteristic lengths in the alternative current perpendicular to plane (CPP) MR are the spin-diffusion lengths in the F and N metals.³ At low temperatures, these are normally long enough to be assumed infinite.³ We⁴ and others^{3,5} have argued that the CPP resistances, R_t , for magnetizations \mathcal{M}_i of neighboring F layers aligned either parallel (P) or antiparallel (AP), should then have simple forms involving only algebraic combinations of independently measured quantities such as the residual resistivities of the N and F metals, ρ_N and ρ_F , and three unknown parameters for a given F/N multilayer that can be found from systematic measurements over ranges of N and F metal thicknesses, t_N and t_F . We should then be able to predict the resistances of any $F1/N/F2/N$ multilayers involving two different F metals in the P and AP states, using only parameters from independent measurements on the separate $F1/N$ and $F2/N$ multilayers. In this paper we examine how well we predict the resistances of sputtered Co/Cu/Ni₈₆Fe₁₄/Cu multilayers, with Co and Ni₈₆Fe₁₄ magnetizations aligned either P or AP to each other, from prior measurements on Co/Cu and Ni₈₄Fe₁₆/Cu, with no adjustable parameters. For brevity, we shorten Ni₈₄Fe₁₆ to Py (≈ permalloy).

The standard models of GMR in both the CPP and CIP geometries assume that the MR results from a reorientation of the \mathcal{M}_i of neighboring F -metal layers from

AP at small applied magnetic field, H , to P above a saturation field, H_s .²⁻⁵ The AP state gives the largest sample resistance and the P state the smallest. The P state can be achieved simply by increasing H to above H_s , where the total magnetization \mathcal{M} becomes maximum.

In contrast, in F/N multilayers with identical F layers and identical N layers, a true AP state occurs only when there is strong enough antiferromagnetic (AF) exchange coupling between neighboring F layers to cause their magnetizations to align AP in zero applied field. For a given t_F , full AF coupling occurs only for a single t_N ,⁶ which seems to give little scope for studying how sample behavior varies as t_N changes. We have argued, however, that, for Co/Ag,⁴ Co/Cu,⁷ and Py/Cu (Ref. 8) multilayers with fixed F thicknesses $t_F \leq 6$ nm, and N thicknesses large enough ($t_N \geq 6$ nm for Co/Cu and Co/Ag and $t_N > 10$ nm for Py/Cu) so that exchange coupling between F layers is weak, the AR_t measured when the sample is first prepared, before any field is applied, often seems to give a good approximation to that of the AP state (see, e.g., the analyses in Ref. 9). We take this state—which we designate H_0 —as the AP state for Co/Cu and Py/Cu in our present analysis. Alternatively, the data and analysis that we present can be viewed as a test of approximating the AP state by the H_0 state.

An AP state can be produced more easily in $F1/N/F2/N$ multilayers, by choosing $F1$ to have a relatively large saturation field, H_{s1} , $F2$ to have a much smaller saturation field, H_{s2} , and t_N to be large enough so that exchange coupling between the $F1$ and $F2$ layers is weak. With such a sample, reducing the applied field from $+H_{s1}$, past zero, to a negative value just beyond $-H_{s2}$, should give an AP state. The samples in this paper contain Co layers with $H_{s1} \approx 100$ – 200 Oe and Py layers with $H_{s2} \leq 10$ Oe.

A sample is shown schematically in Fig. 1(a). To ensure uniform current, the sputtered multilayer of interest is sandwiched between crossed Nb current and voltage strips that superconduct at the measuring temperature of 4.2 K.¹⁰ To avoid proximity effects in the N layers, the first and last layers are Co at least 3 nm thick.¹¹ The sample thus consists of two Nb strips, the multilayer, and

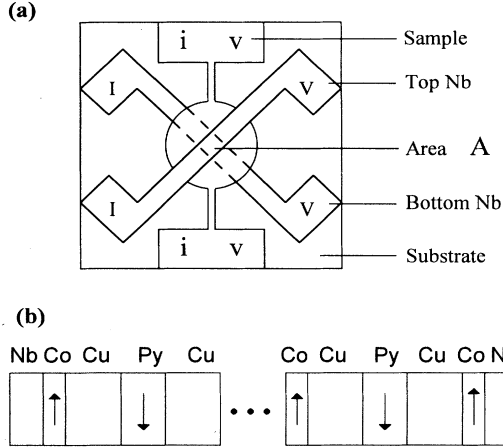


FIG. 1. (a) Sample geometry for simultaneous measurements for CPP (V/I) and CIP (v/i) resistances. The CPP current I flows through the overlap area $A \approx 1.25 \text{ mm}^2$ of the Nb strips. (b) Schematic of the antiparallel (AP) state of Eq. (3).

a “cap” Co layer just below the top Nb strip. In the CPP geometry, we measure the resistance of a unit area, AR_t , the overlap area A of the Nb strips times $V/I = R_t$.

The standard models for the CIP- and CPP-MR divide the current carrying electrons into ones with spin up and ones with spin down.^{2–5} At low temperatures, these electrons should carry current independently, without flipping spins or mixing.³ AR_t is then given simply by a parallel combination of the AR 's for electrons with spin up and down. For CPP data, each AR is, in turn, a series sum of the AR 's for each of the interfaces in the multilayer plus the resistivities times layer thicknesses.^{3–5}

Following Valet and Fert,³ we write the F -metal resistivity as $\rho_F^\uparrow(\rho_F^\downarrow)$ for electron spin along (opposite to) the local F layer magnetization \mathcal{M}_i , and the F/N interface resistance as $R_{F/N}^\uparrow(R_{F/N}^\downarrow)$. We assume spin-independent

Nb/ F interface resistances, $R_{\text{Nb}/F}^\uparrow = R_{\text{Nb}/F}^\downarrow = 2R_{\text{Nb}/F}$, and normal-metal resistivities, $\rho_N^\uparrow = \rho_N^\downarrow = 2\rho_N$, and write $\rho_F^{\uparrow\downarrow} = 2\rho_F^*(1 \mp \beta) = 2\rho_F/(1 \pm \beta)$ and $R_{F/N}^{\uparrow\downarrow} = 2R_{F/N}^*(1 \mp \gamma) = 2R_{F/N}/(1 \pm \gamma)$. $2AR_{\text{Nb}/F}$, ρ_N , $\rho_F^* = \rho_F/(1 - \beta^2)$, $AR_{F/N}^* = AR_{F/N}/(1 - \gamma^2)$, β_F , and $\gamma_{F/N}$ are the parameters of the two-current equations, linear in bilayer number N , derived by Lee *et al.* for simple F/N multilayers:⁴

$$AR_t^{\text{AP}} = 2AR_{\text{Nb}/F} + N\rho_N t_N + N\rho_F^* t_F + 2NAR_{F/N}^*, \quad (1)$$

$$\sqrt{[AR_t^{\text{AP}} - AR_t^{\text{P}}]AR_t^{\text{AP}}} = N[\beta_F \rho_F^* t_F + 2\gamma_{F/N} AR_{F/N}^*]. \quad (2)$$

These equations yield the six parameters each for Co/Cu and Py/Cu.

For a multilayer with N layers of Co/Cu/Py/Cu, AR for the up (+) spin direction and the AP state of Fig. 1(b) is

$$AR^{\text{AP}(+)} = 4AR_{\text{Nb}/\text{Co}} + 4N\rho_{\text{Cu}} t_{\text{Cu}} + (N+1)\rho_{\text{Co}}^\uparrow t_{\text{Co}} + 2NAR_{\text{Co}/\text{Cu}}^\uparrow + N\rho_{\text{Py}}^\downarrow t_{\text{Py}} + 2NAR_{\text{Py}/\text{Cu}}^\downarrow. \quad (3)$$

Substituting in the definitions above gives $AR^{\text{AP}(+)}$ as a function of β and γ . $AR^{\text{AP}(-)}$ is found by replacing \uparrow by \downarrow and vice versa in Eq. (3). Similar expressions can be written for $AR^{\text{P}(+)}$ and $AR^{\text{P}(-)}$, and AR_t^{AP} and AR_t^{P} are then parallel combinations of the appropriate (+) and (–) components.

The bilayer number N , and the layer thicknesses t_{Cu} , t_{Co} , t_{Py} , are chosen for a given sample, and the parameters $2AR_{\text{Nb}/\text{Co}}$, ρ_{Cu} , ρ_{Co} , ρ_{Py} , can all be measured independently of the AR_t 's of Co/Cu, Py/Cu, and Co/Cu/Py/Cu.^{7,8,12,13} Thus, in principle, to calculate AR_t for our Co/Cu/Py/Cu samples, only three “unknowns” each— β_{Co} , $\gamma_{\text{Co}/\text{Cu}}$, $AR_{\text{Co}/\text{Cu}}$, and β_{Py} , $\gamma_{\text{Py}/\text{Cu}}$, $AR_{\text{Py}/\text{Cu}}$ —must be determined from AR_t measurements on Co/Cu and Py/Cu multilayers.

In practice, however, sputtered samples do not give

TABLE I. Fit parameters and independent measurements. (Column 1) Constrained fits to Co/Cu and Py/Cu. (Column 2) Independent measurements of $2AR_{\text{Nb}/\text{Co}}$ (Ref. 12) and $2AR_{\text{Nb}/\text{Py}}$ (Ref. 13) and of ρ_{Co} , ρ_{Py} , and ρ_{Cu} from films sputtered with the Co/Cu and Py/Cu multilayers. (Column 3) Independent measurements of ρ_{Co} , ρ_{Py} , and ρ_{Cu} from films sputtered with the Co/Cu/Py/Cu multilayers.

	Best fit parameters	Indep. meas. Co/Cu;Py/Cu	Indep. meas. Co/Cu/Py/Cu
$2AR_{\text{Nb}/\text{Co}}$ (f Ω m ²)	$6.1^{+1}_{-0.3}$	$6.1^{+1}_{-0.3}$	
$2AR_{\text{Nb}/\text{Py}}$ (f Ω m ²)	7 ± 1.5	$5.7 - 8.5$	
ρ_{Co}^* (n Ω m)	76 ± 5		
$\rho_{\text{Co}} = \rho_{\text{Co}}^* (1 - \beta^2)$	60 ± 9	60 ± 10	51 ± 3
ρ_{Py}^* (n Ω m)	164 ± 20		
$\rho_{\text{Py}} = \rho_{\text{Py}}^* (1 - \beta^2)$	123 ± 40	137 ± 30	111 ± 8
ρ_{Cu} (n Ω m)	4.5 ± 0.5	6 ± 1	5.5 ± 1
β_{Co}	0.46 ± 0.08		
γ_{Co}	0.75 ± 0.05		
β_{Py}	0.50 ± 0.16		
γ_{Py}	0.81 ± 0.12		
$2AR_{\text{Co}/\text{Cu}}^*$ (f Ω m ²)	1.05 ± 0.05		
$2AR_{\text{Co}/\text{Cu}} = 2AR_{\text{Co}/\text{Cu}}^* (1 - \gamma^2)$	0.46 ± 0.10		
$2AR_{\text{Py}/\text{Cu}}^*$ (f Ω m ²)	1.00 ± 0.08		
$2AR_{\text{Py}/\text{Cu}} = 2AR_{\text{Py}/\text{Cu}}^* (1 - \gamma^2)$	0.34 ± 0.22		

precise values for all of these parameters. The data scatter, and independently measured values of $2AR_{\text{Nb/Co}}$, ρ_{Py} , ρ_{Co} , and ρ_{Cu} vary among sputtering runs—e.g., columns 2 and 3 of Table I show that the average resistivities of 300-nm-thick films of Co, Cu, and Py sputtered with Co/Cu/Py/Cu are lower than those previously sputtered with Co/Cu and Py/Cu, although they agree within mutual uncertainties.

Here, we want to see how well we do with no adjustability. We thus fix the Nb/F interface resistances at independently measured values $AR_{\text{Nb/Co}} = 6.1 \text{ f}\Omega \text{ m}^2$,¹² and $AR_{\text{Nb/Py}} = 7 \text{ f}\Omega \text{ m}^2$,¹³ and require all common parameters for Co/Cu, Py/Cu, and Co/Cu/Py/Co to be the same. With these constraints, the remaining parameters are fixed by fits of Eqs. (1) and (2) to the Co/Cu and Py/Cu data.^{13,14}

To justify applying the two-current model for simple AP and P states to our data, we must show that the magnetizations of Co and Py layers reorient at very different fields, and that AR_t and the total magnetization change together. Figure 2 compares magnetization \mathcal{M} versus H [Fig. 2(b)] to AR_t versus H [Fig. 2(a)] for a Co/Cu/Py/Cu (3/20/8/20)₈ multilayer. The lower H_s (Py) layer reorients over a narrow field range near $H=0$, and AR_t increases rapidly over the same range. This narrow range for the Py layers gives a well-defined rise and maximum for AR_t . We designate this maximum as $AR_t(H_{\text{AP}})$. The higher H_s (Co) layer, in contrast, reorients over a much wider field range, giving a near plateau in \mathcal{M} and a nearly flat region in AR_t , followed by a much slower return to saturation. Similar behavior has been seen in CIP measurements on such systems.¹⁵

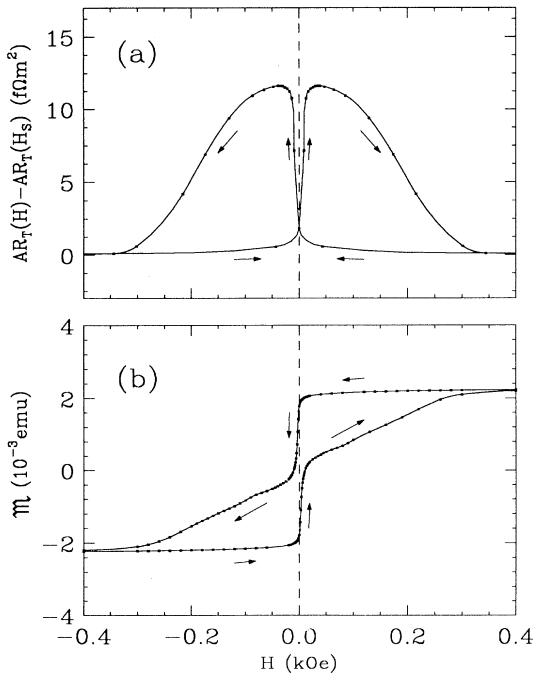


FIG. 2. (a) Magnetoresistance and (b) magnetization \mathcal{M} of a $[\text{Co}(3)/\text{Cu}(20)/\text{Py}(8)/\text{Cu}(20)]_8$ multilayer vs magnetic field H . Sample dimensions are in nm.

We focus on samples with nearly equal Co and Py layer magnetizations (so that the total $\mathcal{M} \approx 0$ for Co and Py magnetizations aligned AP), and with Co and Py thicknesses comparable to those used in the fits.¹⁴ We also focus on Cu layers with $t_{\text{Cu}} = 20 \text{ nm}$, which should be thick enough to make exchange coupling between Co and Py layers weak. A few points with $t_{\text{Cu}} = 10$ and 40 nm show that the results are not sensitive to t_{Cu} .

Figure 3 compares $[\text{Co}(3 \text{ nm})/\text{Cu}(20 \text{ nm})/\text{Py}(8 \text{ nm})/\text{Cu}(20 \text{ nm})]_N$ data with no-adjustable-parameter predictions (solid lines) from the Co/Cu and Py/Cu parameters (column 1 of Table I) obtained as described above. The measuring uncertainties for individual data points are usually dominated by ± 2 –5% uncertainties in the areas A . Reproducibility is indicated by the differences between open and filled symbols, which were sputtered in different runs. The predictions and data agree well at both H_{AP} and H_s . If, instead of the Co/Cu parameters in column 1 of Table I, we start with previously published ones,^{7,8} the agreement is almost as good.¹⁴

A more stringent test of our prediction involves the ratio of the measured and predicted magnetoresistance, $[AR_t(H_{\text{AP}}) - AR_t(H_s)]/[AR_t^{\text{AP}} - AR_t^{\text{P}}]$. The ratios for the data and predictions of Fig. 3 range from 1.1–1.3 and average about 1.2 instead of 1. Given the constraints placed on the fits, this agreement is rather good. The fit in Fig. 3 can be improved, giving a ratio average of about 1.1, by increasing the values of ρ_{Py}^* , β_{Py} , and β_{Co} , within their uncertainties.

We conclude that the rather good agreement in Fig. 3 between the no-free-parameter predictions and our data provides important new evidence that low-temperature CPP data for magnetic multilayers can be described by a simple, independent two-current model that contains no

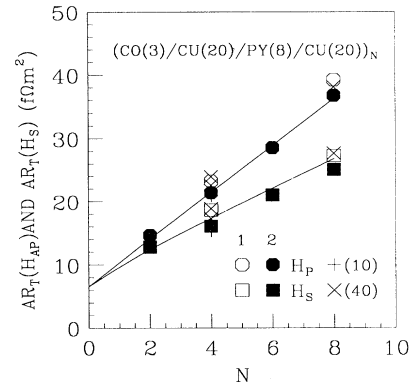


FIG. 3. $AR_t(H_{\text{AP}})$ and $AR_t(H_s)$ for $[\text{Co}(3)/\text{Cu}(20)/\text{Py}(8)/\text{Cu}(20)]_N$ multilayers for $N=2, 4, 6, 8$. For $t_{\text{Cu}} = 20 \text{ nm}$, the solid lines are for the parameters in column 1, Table I. Open and filled symbols for $N=4$ and 8 are for samples from different sputtering runs; their differences show our reproducibility. The crosses are for samples with $t_{\text{Cu}} = 40 \text{ nm}$ and the pluses for $t_{\text{Cu}} = 10 \text{ nm}$. With $\rho_{\text{Cu}} \approx 5 \text{ n}\Omega \text{ m}$, the changes in AR_t from $t_{\text{Cu}} = 20 \text{ nm}$ to 10 nm or 4 nm are $\approx -0.1N \text{ f}\Omega \text{ m}^2$ and $+0.2N \text{ f}\Omega \text{ m}^2$, respectively. Even for $N=8$, these are only ≈ -0.8 and $+1.6 \text{ f}\Omega \text{ m}^2$, about our reproducibilities.

lengths other than the thicknesses of the constituent layers.³⁻⁵ The agreement also supports our argument^{4,9} that the H_0 state resistances of our Co/Cu, and Py/Cu multilayers lie near those for AP F -layer alignment.

The research was supported by part by the NSF under Grant No. DMR-92-22614, by the MSU Center for Fundamental Materials Research, and by the Ford Motor Co.

¹L. Falicov *et al.*, *J. Mater. Res.* **5**, 1299 (1990).

²See, e.g., J. Barnas *et al.*, *Phys. Rev. B* **42**, 8110 (1990).

³T. Valet and A. Fert, *J. Magn. Magn. Mater.* **121**, 378 (1993); *Phys. Rev. B* **48**, 7099 (1993).

⁴S.-F. Lee *et al.*, *J. Magn. Magn. Mater.* **118**, L1 (1993).

⁵S. Zhang and P. M. Levy, *J. Appl. Phys.* **69**, 4786 (1991).

⁶See, e.g., S. S. P. Parkin *et al.*, *Phys. Rev. Lett.* **64**, 2304 (1990); D. H. Mosca *et al.*, *J. Magn. Magn. Mater.* **94**, L1 (1991).

⁷W. P. Pratt, Jr. *et al.*, *J. Magn. Magn. Mater.* **126**, 406 (1993).

⁸P. A. Schroeder *et al.*, in *Magnetic Ultrathin Films: Multilayers and Surfaces/Interfaces and Characterization*, edited by B. T. Jonker, S. A. Chambers, R. F. C. Farrow, C. Chappert, R. Clarke, W. J. M. de Jonge, T. Egami, P. Grünberg, K. M. Krishnan, E. E. Marinero, C. Rau, and S. Tsunashima, MRS Symposia Proceedings No. 313 (Materials Research Society, Pittsburgh, 1993), p. 47.

⁹P. A. Schroeder *et al.*, in *Magnetism and Structure in Systems of Reduced Dimension*, Vol. 309 of *NATO Advanced Study Institute, Series B: Physics*, edited by R. F. C. Farrow, B. Dieny,

M. Donath, A. Fert, and B. D. Hermsmeier (Plenum, New York, 1993), p. 129; P. A. Schroeder *et al.*, *J. Appl. Phys.* (to be published).

¹⁰W. P. Pratt *et al.*, *Phys. Rev. Lett.* **66**, 3060 (1991).

¹¹J. M. Slaughter *et al.*, *Proceedings of LT-18* [Jpn. J. Appl. Phys. **26**, Suppl. 26-3, 1451 (1987)].

¹²C. Fierz *et al.*, *J. Phys. Condens. Matter* **2**, 9701 (1990).

¹³P. Holody *et al.* (unpublished); Q. Yang *et al.* (unpublished).

¹⁴The Co/Cu data involve 27 pairs of H_0 and H_s values in three sets, all with total thickness $t_T = 720$ nm: (a) $t_{Co} = 1.5$ nm, (b) $t_{Co} = 6$ nm; and (c) $t_{Co} = t_{Cu}$ (Refs. 8, 9, and 13). The Py/Cu data consist of 16 pairs of H_0 and H_s values in two sets, all with $t_t = 360$ nm: (a) $t_{Py} = 1.5$ nm; (b) $t_{Py} = 6$ nm (Refs. 9 and 13). One Py/Cu pair was excluded because *both* points fall far above the others (Ref. 13). Including them greatly increase χ^2 .

¹⁵See, e.g., B. Dieny *et al.*, *J. Appl. Phys.* **69**, 4774 (1991); A. Chaiken *et al.*, *Appl. Phys. Lett.* **59**, 240 (1991); H. Yamamoto *et al.*, *J. Magn. Magn. Mater.* **126**, 437 (1993).